JOURNAL OF APPLIED ELECTROCHEMISTRY **21** (1991) 130–135

The manganese dioxide electrode
Part XI: an X-ray diffraction study of materials produced by H insertion into an EMD

J. FITZPATRICK, F. L. TYE

Energy Technology Centre, Middlesex Polytechnic, Bounds Green Road, London N11 2NQ, UK

Received 24 February 1990; revised 18 May 1990

Thirty-one samples of composition $MnOOH_r$, where $0.1 < r < 1.0$, were prepared under mild conditions by reacting a commercial electrodeposited manganese dioxide (EMD) with xylene, acetone, cinnamyl alcohol or combinations thereof. Although the X-ray pattern reflected the expected dilation of the crystal structure in the region $0.1 < r < 0.8$ the attainment of an H insertion level of $MnOOH_{0.8}$ without the emergence of additional peaks is a new finding. The expansion was nearly isotropic and careful examination of peak positions and intensities indicated changes in behaviour at about $r = 0.25$ and 0.45. Another finding was the ability of inserted H to migrate across the boundaries of nominally dry powders in the region $0.1 < r < 0.8$. In the region $r > 0.8$ expansion was clearly anisotropic and as a consequence new diffraction peaks emerged and some of the peaks present at lower H insertion levels were substantially reduced in intensity. A particularly important observation was the restricted mobility shown by inserted H in the end-product MnOOH as this has implications for the performance of EMD in batteries. The X-ray diffraction pattern of the end-product was dissimilar to α- and γ-MnOOH in important respects and a previous suggestion that it is called δ-MnOOH seems preferable.

1. Introduction

Manganese dioxide is the positive active material used in Leclanché and alkaline manganese batteries [1] which together dominate the primary battery market. Synthetic manganese dioxides and particularly those made by electrodeposition are used in high performance batteries. It is now widely accepted that manganese dioxide discharges by abstraction of H^+ from the electrolyte and reception of electrons from the external circuit via carbon black or graphite conductors [2]. The reaction may be conveniently represented as follows

$$MnOOH_r + \Delta H^+ + \Delta e \longrightarrow MnOOH_{r+\Delta}$$

where r represents the level of H insertion which changes from about 0.1 in the starting material to 1.0 at the theoretical completion of discharge.

Although many worthwhile investigations have been carried out on MnO_2–H insertion compounds, some have used materials not employed in batteries and all have been limited to relatively few levels of H insertion. X-ray diffraction has proved to be a powerful technique in this field and the purpose of this paper is to report the findings of a powder X-ray diffraction study on a manganese dioxide used in batteries at 31 levels of H insertion.

2. Experimental

The starting material was a commercial electrodeposited manganese dioxide of composition $MnOOH_{0.11}$ which has been used in many previous investigations [3–12] and is coded R2. R2 consists of 93.4% $MnO_{1.95}$ and 4.33% combined water evolved between 110 and 1000° C [34]. Based on a nitrogen adsorption/desorption study the material has been described as a non-rigid structure with platelets or flakes held apart at maximum contraction by the edges of neighbouring platelets or by debris [35]. It has BET surface area of $38\,m^2\,g^{-1}$ [35] and if sintered at 280° C to induce rigidity has a pore volume of $0.046\,cm^3\,g^{-1}$ [35].

A non-aqueous reduction medium was preferred for the reasons given in the next section. A new finding was that not only cinnamyl alcohol but also xylene which was used previously as an inert solvent and acetone caused reduction. The order of reactivity was

$$\text{xylene} < \text{cinnamyl alcohol (dissolved in xylene)} < \text{acetone}$$

With xylene, very long times were required at ambient temperature to achieve high degrees of reduction, for example, nine months immersion yielded a product of composition $MnOOH_{0.89}$. This is a likely consequence of the difficulty of abstracting H from a stable aromatic compound. The reactivity of manganese dioxide with organic substances will not surprise those familiar with the excellent reviews of Fatiadi [13].

The three reductants were used individually and in combination under mild conditions, i.e. no heating above 40° C and with cooling when appropriate. The final processes were an acetone wash, air drying and a

0021-891X/91 $03.00 + .12

prolonged period of storage in an air-tight bottle. Fifty three samples were prepared from which thirty one were selected to cover the range $0.1 \leqslant r \leqslant 1.0$. The values of r in $MnOOH_r$ were determined by the potentiometric method of Vetter and Jaeger [14].

Powder X-ray diffraction was carried out with the following equipment supplied by Philips: PW 1730/10 high performance 4 kW 60 kV constant potential generator; PW 2253/20 broad focus copper anode X-ray tube; PW 1050/81 goniometer and step motor; PW 1710/00 diffractometer control; PW1752/00 graphite monochromator; PW 1711/10 xenon proportional counter.

The operating conditions for traced patterns were: generator set at 45 kV and 60 mA; goniometer scan speed of 0.02° of 2θ per second; chart recorder speed of 10 mm per degree of 2θ; proportional counter pulse height selection set between 35 and 70%; counter time constant of 2 s; and diffractometer settings of 1° for the divergence and scatter slits and 0.2 mm for the receiving slit.

More precise location of peak maxima and estimation of peak intensities were achieved by a programme which sampled the counts for 10 s in steps of 0.01° of 2θ for 0.2° of 2θ on either side of the peak position estimated from a chart, and calculated the moving average for three successive samples. For the broad peak at about 2θ 22° the step scan was extended to 0.4° of 2θ on either side of the estimated chart peak. All samples for X-ray diffraction were ground in an agate mortar for 10 min and mounted into the aluminium sample holders by backfilling against glass slides. Interplanar spacings were calculated from 2θ values using the Bragg equation in the form

$$\text{Interplanar spacing} = 0.0771/\sin\theta$$

where the interplanar spacing is in nanometres and θ is in degrees.

3. Results and discussion

Whilst a chemical process for insertion of H into manganese dioxide has obvious advantages over an electrochemical procedure in terms of the absence of complicating phases such as the electronic conductor and zinc compounds, there is one inherent difficulty which is often ignored. Irrespective of whether the rate of H insertion is controlled by diffusion of reactants or products in the liquid phase or solid phase or by the transformation of an activated complex at the interface between the phases, it is inevitable that the particles with the higher surface to volume ratio will receive the greater amount of H insertion per unit weight. In other words all chemical processes must result in r in $MnOOH_r$ being higher initially for the smaller particles. Equalization of r among particles of different sizes may occur as a consequence of subsequent processes.

In aqueous environments equilibrium between different sizes of particles may be reached via the intervention of soluble manganese species. This, however, is a further complication as it may lead to the appearance of a phase and to behaviour which is not characteristic of the H insertion compound. The use of hydrazine in 30 wt% KOH, for example, led to the consumption of the smallest particles and to the deposition of δ-MnO_2 on the surface of the larger particles [15]. Non aqueous reduction media were therefore chosen for this study. Separate analyses were carried out to establish that no soluble manganese could be detected in the liquid media.

Fortunately a simple unambiguous experiment has shown that the inserted H migrates across the particle interfaces of nominally dry powders. This process ensures uniform H insertion among equilibrated particles of different sizes and is the reason for the prolonged storage pretreatment used in this investigation. The evidence for this migration is given in Fig. 1. This figure shows how the X-ray diffraction pattern of a mixture containing equal amounts of $MnOOH_{0.11}$ and $MnOOH_{0.66}$ firmly packed in a sample holder [36] developed with time. The initial pattern shows the twin peaks expected of a mixture of materials having two H insertion levels. As time progressed the peaks gradually coalesced until after 18 days the normal five peak pattern was obtained. This must have occurred as a result of the migration of H from the $MnOOH_{0.66}$ compound to the $MnOOH_{0.11}$ compound. Figure 2 compares the X-ray pattern of the 50%–50% mixture of $MnOOH_{0.11}$ and $MnOOH_{0.66}$ after 61 days with a preparation of composition $MnOOH_{0.38}$. The peak positions were identical. Such a result is consistent with the principal driving force for this change being a H diffusion gradient in the solid state which led to a uniform H distribution throughout the material.

Figure 3 compares the X-ray diffraction patterns of the starting material $MnOOH_{0.11}$ with $MnOOH_{0.80}$.

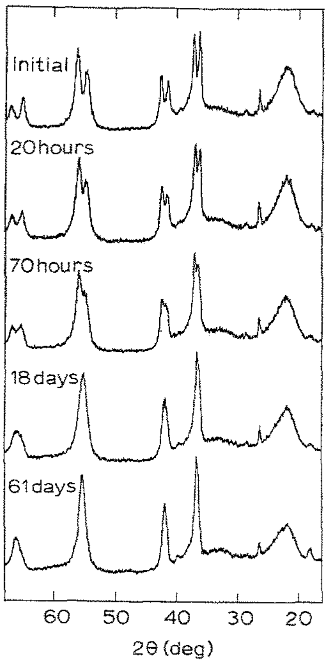

Fig. 1. X-ray diffraction patterns of a 50%–50% mixture of $MnOOH_{0.11}$ and $MnOOH_{0.66}$ as a function of time.

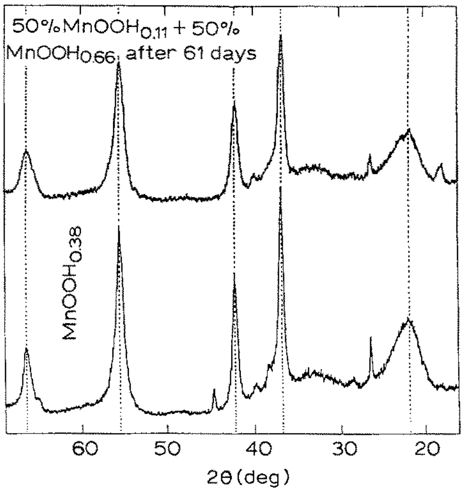

Fig. 2. Comparison of the X-ray diffraction pattern of a 50%–50% mixture of $MnOOH_{0.11}$ and $MnOOH_{0.66}$ after 61 days with that for $MnOOH_{0.38}$.

The insertion of H up to $r = 0.80$ clearly proceeded without any change in the main features of the diffraction pattern except the well-known movement of peak positions due to lattice dilation [16–22] and some changes in intensity. As far as the authors are aware $MnOOH_{0.8}$ is the highest H insertion that has been achieved without the emergence of additional diffraction peaks. This result is attributed to the non-aqueous environment and possibly also to the mild conditions which were used in the preparation of the H insertion compounds. It is interesting that the small peak F also shifted and must be regarded therefore as originating from the same expanding crystal structure. A few minor peaks in Fig. 3 did not move with H insertion. Those at 2θ 38.3° and 44.6° were due to the aluminium sample holder and that at 2θ 26.5° was due to carbon impurity in the electrodeposited manganese dioxide.

At insertion values greater than $r = 0.8$ the X-ray diffraction pattern changed in character. This is illustrated in Fig. 4 which compares the patterns of $MnOOH_{0.8}$ and $MnOOH_{1.01}$. Peaks A, C and D decreased substantially in intensity and new peaks G, H, I and J emerged. Although as is shown in Fig. 5 the new peaks G, H, I and J correspond to peaks in the γ-MnOOH pattern [23], the absence of the strongest γ-MnOOH peak at 2θ 26.1° and the continued presence at undiminished intensity of Peak E which is not present in γ-MnOOH make it unlikely that there was a significant amount of recrystallization to γ-MnOOH in the region $r > 0.8$. On the other hand Fig. 6 shows that the X-ray diffraction pattern of $MnOOH_{1.01}$ has little correspondence with the published pattern of α-MnOOH [24]. The conclusions of previous workers that the end product of H insertion is α-MnOOH [20, 21, 25–29] or a mixture of α- and γ-MnOOH [30] are therefore not supported by this investigation. Attempts to cause the diffraction pattern to change at lower H insertion levels, i.e. $r < 0.8$ by refluxing samples in xylene at 138° for 5 h, failed. It is particularly noteworthy, as shown in Fig. 4, that in the region $r > 0.8$, peaks B, C and D continued to shift to lower angles as H insertion increased. This behaviour is compatible with a conclusion that the solid solution extended over the complete range $0.1 < r < 1.0$. Furthermore as the end product appears to be neither γ- nor α-MnOOH, the earlier suggestion that it should be distinguished from these compounds by calling it δ-MnOOH [22] seems appropriate.

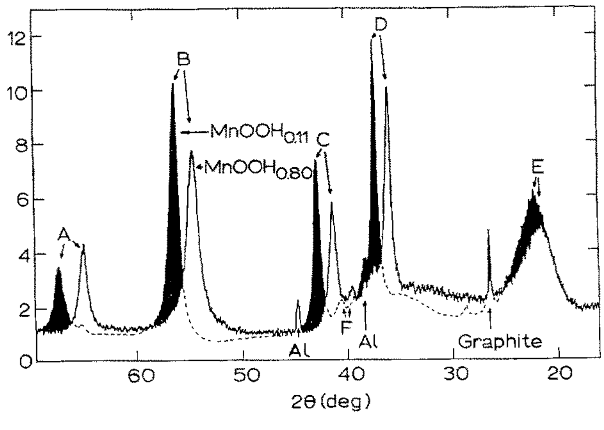

Fig. 3. Comparison of the X-ray diffraction patterns of $MnOOH_{0.11}$ and $MnOOH_{0.80}$.

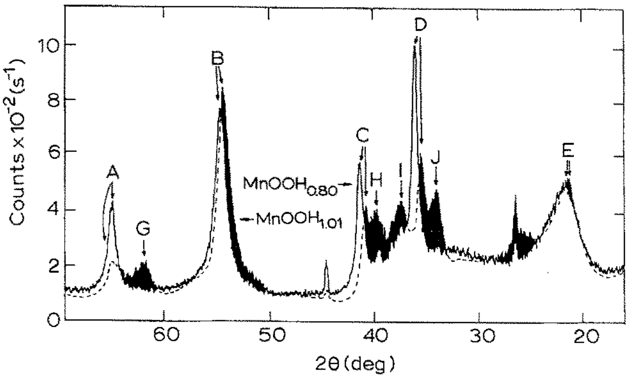

Fig. 4. Comparison of the X-ray diffraction patterns $MnOOH_{0.80}$ and $MnOOH_{1.01}$.

If the dilation caused by H insertion were isotropic then the ratio of any two interplanar spacings would be constant and independent of the level of H insertion. All six ratios derived from peaks A, B, C and D are presented as a function of r in Fig. 7. Peak E was not used because its breadth precluded accurate estimation of the associated interplanar spacing. Figure 7 shows that expansion was isotropic to within 1% up to a H

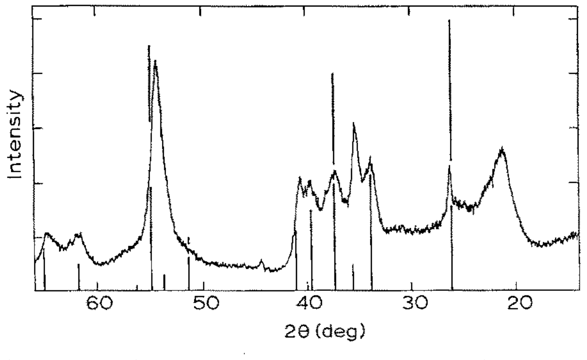

Fig. 5. Comparison of the X-ray diffraction pattern of $MnOOH_{1.01}$ with the JCPDS pattern for γ-MnOOH.

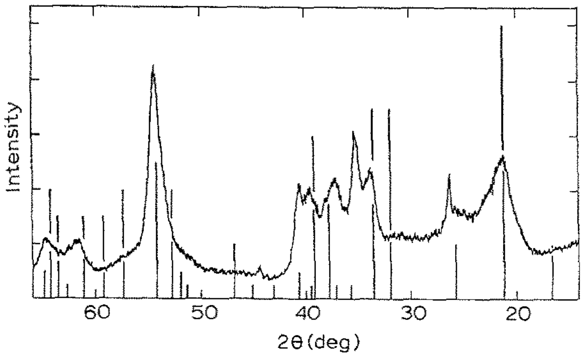

Fig. 6. Comparison of the X-ray diffraction pattern of $MnOOH_{1.01}$ with the JCPDS pattern for α-MnOOH.

insertion level of $r = 0.8$. At higher insertion levels than this the interplanar spacings derived from peaks C and D increased more rapidly than those derived from peaks A and B. Thus in the region $r > 0.8$ dilation was clearly anisotropic. It seems probable that the new peaks G, H, I and J which emerged in this region were a consequence of the anisotropic expansion changing the symmetry of the crystal structure.

Even in the region $r < 0.8$ slight trends in the interplanar spacing ratios which were greater than experimental error are observable in Fig. 7. For example the interplanar spacing ratios derived from peak B/peak A increased at first with r and then decreased. The converse applies for the ratio derived from peak D/peak B. Thus even in the region $r < 0.8$ the shape of the unit cell must have been changing slightly with H insertion. Figure 8 shows plots of the individual interplanar spacings derived from peaks A, B, C and D. The higher rate of dilation with increasing H insertion for peaks C and D in the region $0.8 < r < 1.0$ is clearly evident. Peaks B and C in particular also appear to show a change in the dilation rate at about the mid-reduction point. Figure 8 is also drawn to indicate that another change in the rate of dilation took place at $r = 0.25$. The justification for suggesting a change at this level of H insertion is strengthened when peak heights are considered.

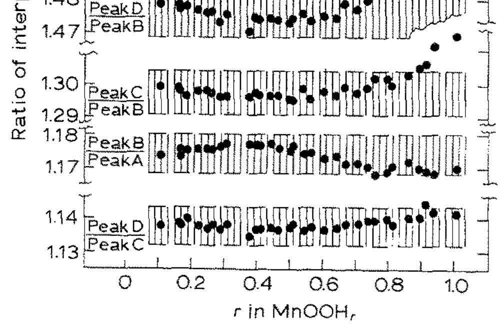

Fig. 7. Interplanar spacing ratios versus H insertion level.

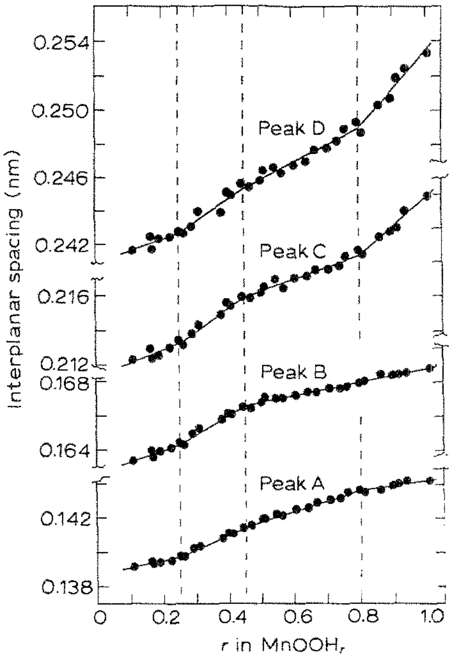

Fig. 8. Interplanar spacing against H insertion level.

Reproducible peak heights and integrated peak intensities are experimentally difficult to achieve. The factors responsible for variability include, changes in the performance of the X-ray source, variations in the particle size distribution, differences in the packing of the sample in the holder, and statistical errors arising from the detection procedure. Examination of the diffraction patterns revealed that, in general, all the peaks in a particular pattern were either high or low or in between. In other words the circumstance that one peak in a pattern would be higher than normal while another peak was lower than normal did not arise. This observation indicated that smoothing of the peak height data by a normalizing process would be valid. Peak A was chosen for normalization because, as is shown in Fig. 9, the height of this peak appeared to be independent of H insertion level in the region $0.1 < r < 0.8$. The line drawn on Fig. 9 denotes the smoothed peak height values, $\bar{h}$, used for peak A in normalization. The normalized heights of other peaks were calculated using the relationship

$$\text{Normalized height of peak X} = \frac{\bar{h} \times \text{height of peak X}}{\text{height of peak A}}$$

Figure 10 shows plots of normalized peak heights

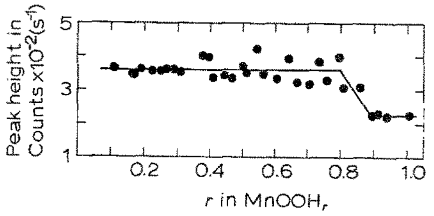

Fig. 9. Height of peak A against H insertion level.

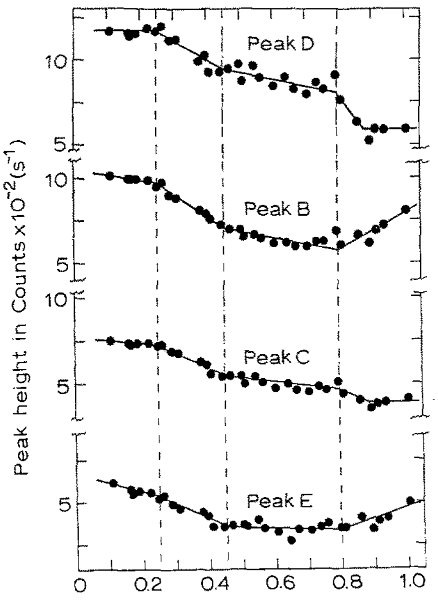

Fig. 10. Normalized peak height against H insertion level.

against the level of H insertion. The existence of a change at about $r = 0.25$ is now obvious particularly for peaks B and D and the change at about the mid-reduction point is confirmed. A fairly sharp and substantial decrease in peak height occurs in the region $0.8 < r < 0.9$ for peak D and as is shown in Fig. 9 for peak A. A similar but less substantial decrease in peak height may occur for peak C. These changes were noted earlier in connection with Fig. 4 and are consistent with a change in symmetry causing peak splitting.

The migration of H across interparticulate boundaries in order to achieve the same level of H insertion in two materials was demonstrated with $MnOOH_{0.11}$ and $MnOOH_{0.66}$ and is illustrated in Fig. 1. Figure 11 shows the movement of peaks for a 50%–50% mixture of the starting and most reduced materials, i.e. $MnOOH_{0.11}$ and $MnOOH_{1.01}$, firmly packed in a sample holder. Although peaks A, B, C and D of the starting materials and peaks A′, B′, C′ and D′ of the most reduced material moved closer together with time indicating some migration of inserted H, the amount of migration was limited. Even after 447 days, coalescence of the peaks, which would have indicated the attainment of the same level of H insertion in the two materials, was not observed. The diminution in the intensities of the new peaks G, H, and J on contact with the starting material as is shown in Fig. 11 is indicative that these peaks are properly part of the solid solution system. However, their continued presence even after very prolonged contact with the starting material is further evidence of a restriction to H migration. From the positions of peaks A, B, C and D in the mixture and Fig. 8 it was possible to calculate the amount of H received by the material which had a composition of $MnOOH_{0.11}$ at zero time. The results, which are shown in Fig. 12, confirm that although the initial migration of H occurred relatively rapidly the anticipated content of inserted H was not achieved even after very long times. The inference that in the region $0.8 < r < 1.0$ the migration of inserted H may be inhibited has important implications for the performance of batteries and their energy yield.

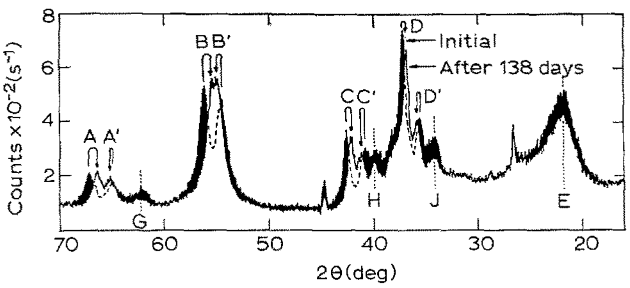

Fig. 11. Comparison of the X-ray diffraction patterns of a 50%–50% mixture of $MnOOH_{0.11}$ and $MnOOH_{1.01}$ initially and after 138 days.

4. Summary

As H was chemically inserted into a commercial electrodeposited manganese dioxide, the crystal structure dilated and the intensities of five main peaks changed. Expansion occurred anisotropically although in the region $0.1 < r < 0.8$ it was nearly isotropic. Changes in behaviour were discernible at three levels of H insertion: $r = 0.25$, 0.45 and 0.80.

In the region $0.1 < r < 0.25$ peak heights remained reasonably constant. However slight anisotropic expansion would be expected to cause stresses at crystal boundaries and it is speculated that at $r = 0.25$ the stresses were relieved by the generation of enlarged regions of disorder between crystallites with concomitant reductions in crystallite size. Once this process had started dilation was able to occur more rapidly, and peak heights fell due to the generation of larger amounts of disorder between the crystallites which became smaller in consequence. This is the presumed explanation of behaviour in the region $0.25 < r < 0.45$.

The change at $r = 0.45$ confirms changes that have been observed in other phenomena at about the mid-reduction point [31]. These have been attributed to changes in the type of site occupied by the inserted species [31, 32] and hence to a change in configurational entropy of the inserted species [32, 33].

Finally in the region $0.8 < r < 1.0$ the expansion generated by the inserted H (or more accurately

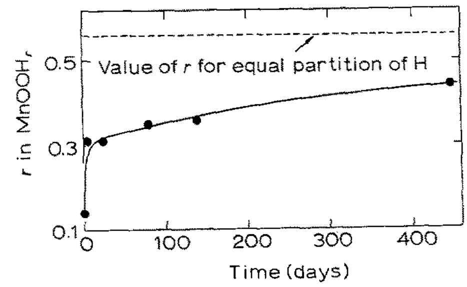

Fig. 12. Increase in the H insertion level of $MnOOH_{0.11}$, as a result of H migration from $MnOOH_{1.01}$ in 50%–50% mixture, as a function of time.

generated by the reduction of positive charge on the manganese ion) caused the unit cell to change shape. In consequence peaks A, C and D decreased in intensity and four new peaks appeared. The change in unit cell shape was accompanied by a dramatic reduction in the mobility of about half of the inserted H.

The X-ray diffraction pattern of the end-product is dissimilar to both α-MnOOH and γ-MnOOH in important respects and a previous suggestion that it is termed δ-MnOOH seems preferable.

Acknowledgements

The authors wish to thank SERC and Ever Ready Ltd. for their financial support toward this investigation.

References

[1] F. L. Tye, ‘Electrochemical Power Sources’, (edited by M. Barak), Peter Peregrinus, London (1980) p. 50.

[2] F. L. Tye, Proc. 7th Australian Electrochem. Conf., (edited by T. Tran and M. Skyllas-Kazacos), The Royal Australian Chemical Institute (1988) p. 37.

[3] J. Muller, F. L. Tye and L. L. Wood, ‘Batteries’, Vol. 2, (edited by D. H. Collins), Pergamon, London (1965) p. 201.

[4] J. Caudle, K. G. Summer and F. L. Tye, *J. Chem. Soc. Faraday Trans. I* **69** (1973) 876.

[5] *Idem, ibid.* **69** (1973) 885.

[6] J. A. Lee, C. E. Newnham, F. S. Stone and F. L. Tye, *J. Colloid and Interfac. Sci.* **45** (1973) 289.

[7] A. J. Brown, C. R. St. Claire-Smith, F. L. Tye and J. L. Whiteman, *ibid.* **51** (1975) 516.

[8] J. A. Lee, C. E. Newnham, F. L. Tye and F. S. Stone, *J. Chem. Soc. Faraday Trans. I* **74** (1978) 237.

[9] A. Agopsowicz, J. L. Hitchcock and F. L. Tye, *Thermochim. Acta* **32** (1979) 63.

[10] A. J. Brown, F. L. Tye and L. L. Wood, *J. Electroanal. Chem.* **122** (1981) 337.

[11] W. C. Maskell, J. E. A. Shaw and F. L. Tye, *Electrochim. Acta* **26** (1981) 1403.

[12] W. C. Maskell, J. E. A. Shaw and F. L. Tye, *J. Power Sources* **8** (1982) 113.

[13] A. J. Fatiadi, *Synthesis* **8** (1976) 65 and 133.

[14] K. T. Vetter and N. Jaeger, *Electrochim. Acta* **11** (1966) 401.

[15] D. M. Holton, W. C. Maskell and F. L. Tye, ‘Power Sources 10’, (edited by L. Pearce), The Paul Press (1985) p. 247.

[16] J. Brenet, J. Mallessan and A. Grund, *C.R. Acad. Sci.* **242** (1956) 111.

[17] J. Brenet, ‘8^{e} Reunion du CITCE Madrid 1956’, Butterworths, London (1957) p. 394.

[18] K. Neumann and W. Fink, *Zeit Elektrochem.* **62** (1958) 114.

[19] W. Feitknecht, H. R. Oswald and U. Feitknecht-Steinmann, *Helv. Chim. Acta* **43** (1960) 1947.

[20] J. P. Gabano, B. Morignat, E. Fialdes, B. Emery and J. F. Laurent, *Zeit. Phys. Chem.* **46** (1965) 359.

[21] J. A. Lee, C. E. Newnham, F. L. Tye and F. S. Stone, *J. Chem. Soc. Faraday Trans. I* **74** (1978) 237.

[22] W. C. Maskell, J. E. A. Shaw and F. L. Tye, *Electrochim. Acta* **26** (1981) 1403.

[23] JCPDS 18 – 805.

[24] JCPDS 12 – 733.

[25] H. Bode, A. Schmier and D. Berndt, *Zeit. Elektrochem.* **66** (1962) 586.

[26] *Idem, ibid.* **68** (1965) 106.

[27] J. F. Laurent and B. Marignat, ‘Batteries’, (edited by D. H. Collins), Pergamon, London (1963) p. 309.

[28] R. Giovanoli, K. Bernhard and W. Feitknecht, *Helv. Chim. Acta* **51** (1968) 355.

[29] M. Beley and J. Brenet, *Electrochim Acta* **18** (1973) 1003.

[30] T. Ohzuku and T. Hirai, ‘Manganese Dioxide Electrode Theory and Practice for Electrochemical Applications’, (edited by B. Schumm, R. L. Middaugh, M. P. Grotheer and J. C. Hunter), The Electrochem. Soc., Pennington, New Jersey (1985) p. 141.

[31] W. C. Maskell, J. E. A. Shaw and F. L. Tye, *J. Applied Electrochem.* **12** (1982) 101.

[32] F. L. Tye, *Electrochim. Acta* **30** (1985) 17.

[33] W. C. Maskell, J. E. A. Shaw and F. L. Tye, *ibid.* **28** (1983) 225.

[34] D. S. Freeman, P. F. Pelter, F. L. Tye and L. L. Wood, *J. Applied Electrochem.* **1** (1971) 127.

[35] C. St Claire-Smith, J. A. Lee and F. L. Tye, ‘Manganese Dioxide Symposium’, Vol. 1, Cleveland, (edited by A. Kozawa and R. J. Brodd), I.C. Sample Office (1975) p. 132.

[36] D. G Malpas and F. L. Tye, ‘Handbook of Manganese Dioxides Battery Grade’, (edited by D. Glover, B. Schumm and A. Kozawa), International Battery Material Association, Brunswick, Ohio, USA (1989) p. 177.